



## Simple and accurate estimation of metal, semiconductor, and insulator work functions

Zeyu Jiang, Damien West, and Shengbai Zhang <sup>\*</sup>

*Department of Physics, Applied Physics and Astronomy, Rensselaer Polytechnic Institute, Troy, New York 12180, USA*

 (Received 8 July 2022; revised 18 October 2022; accepted 5 January 2023; published 19 January 2023)

Work-function  $\phi$  measures the work needed for an electron to escape a solid. For simple metals, it is almost exclusively the result of the surface dipole created by spill-out of electrons from bulk into the vacuum as shown in the seminal work by Lang and Kohn [*Phys. Rev. B* **3**, 1215 (1971)] using a jellium model. Despite a half century of intense efforts, however, such understanding has not been extended past metals. Here we present a universal model for  $\phi$  which contains a previously unrecognized bulk contribution  $\phi_I$  [*Phys. Rev. Lett.* **121**, 196802 (2018)]. By incorporating  $\phi_I$  into the jellium model, we find that it dictates the dipole due to charge spill out and provides a description which applies to a wide range of materials, ranging from metals, semiconductors, to insulators.

DOI: [10.1103/PhysRevMaterials.7.015001](https://doi.org/10.1103/PhysRevMaterials.7.015001)

### I. INTRODUCTION

Work function is a key part of the original theory of Einstein on photoelectric effect [1]. Its importance to science spans a wide range of topics from thermionic emission and energy conversion [2], chemisorption [3], surface reconstruction [3], surface chemistry [4], chemical sensors [5], material's fracture toughness [6] and mechanical strength [7], to free-electron lasers [8], to name a few. In the context of the so-called Schottky-Mott limit [9,10] and Anderson rule [11], the work function also serves as a rough guide to band alignment for electronic device design [12,13], interfacial diagnosis [14], and to match redox potentials for photoelectrochemical reaction and energy conversion [15].

On the theoretical side, density functional theory- (DFT-) based methods provide reliable access to accurate results of work functions [16], using a periodic supercell with “slab plus vacuum” geometry. In addition to the work function, Schottky barriers between lattice-matched heterostructures are routinely calculated [17]. Such calculations determine the interfacial dipoles and show that the interfacial properties between materials cannot be reduced to their constituent parts as in the Schottky-Mott limit or Anderson rule [18]. Although these calculations provide quantitative results, they provide little understanding on the physics and factors that control the alignment at material interface. As such, a basic understanding of interfacial dipole formation, or even what constitutes the interfacial dipole, which could serve as a foundation for understanding material interfaces without explicit atomistic calculation is still lacking.

A general model of the surface work function, which can be thought of as the extreme case of an interface, was proposed by Lang and Kohn (LK) [19] in which they postulate that the crystalline details are unimportant, and the ionic potential can be replaced by that of a uniform background

charge. Such a jellium model provides reasonable results for simple metals but has failed for semiconductors and insulators. This leads to the question of whether a fully atomistic calculation is necessary to capture the essential physics of nonmetals, or if instead a hidden physical property can be included in a simple model to cover a broad range of materials.

The difficulty in the description of the work function partly comes from that most of our understanding of solids are based on the construct of periodic bulk system, thanks to the Bloch theorem and to the wide adoption of Fourier transform. In this regard, the surface can be viewed as follows: first the infinitely large periodic bulk forms an interface with the “empty space” of vacuum, and second this interface reaches equilibrium by creating surface relaxation dipoles. Yet, one always needs a common reference to quantify interactions and align electronic levels between subsystems when placed together. For example, in quantum chemistry, the reference of a molecule is chosen as the position infinitely far away from the molecule. An obvious drawback of the periodic bulk theory is that the reference gets “lost,” between the bulk and the vacuum since there is no “infinitely far” position for an infinitely large bulk. Without identifying the reference for periodic bulk, we do not know how to properly define the surface and its relaxation.

In this paper, we formulate a theory of work function and show that the bulk ideal vacuum level [20] plays a critical role in determining the overall work function. As atomic surface relaxation can be trivially incorporated, here we only consider the effect on the work function due to electronic relaxation. This work function contains two parts: a pure bulk term  $\phi_I$  dubbed as the innate bulk work function and a surface-relaxation dipole term  $V_{D_R}$ . The bulk contribution  $\phi_I$  is the Fermi-level position (or the valence-band maximum for the case of nonmetals) relative to the ideal vacuum level. By a real-space charge and potential analysis, we show that  $V_{D_R}$  can be evaluated using a corrected jellium model based on Lang and Kohn's approach [19], provided that the effect of  $\phi_I$  is incorporated. The results are compared with first-principles atomistic calculations for 21 real solids. Good agreement is

<sup>\*</sup>zhangs9@rpi.edu

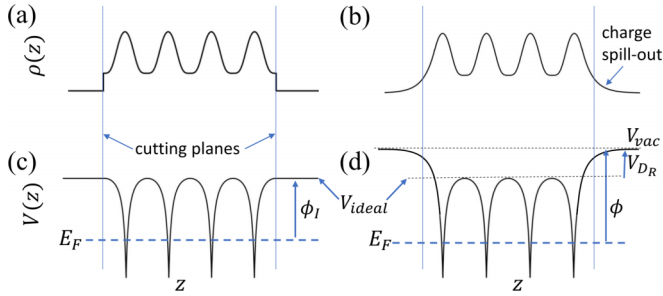


FIG. 1. Schematic of the charge density of a truncated slab with the cutting planes depicted as vertical lines, (a) before and (b) after electronic relaxation. The electrostatic potential corresponding to the charge densities in (a) and (b) are shown in (c) and (d), respectively.

found across the board for metals, semiconductors, and insulators, leading to a universal description of the work function.

## II. MODEL ANALYSIS

### A. Bulk and surface contribution to the work function

In general, the work-function  $\phi^{\hat{n}}$  of a solid is a direction-dependent ( $\hat{n}$ ) quantity defined by the difference between the vacuum potential  $V_{\text{vac}}^{\hat{n}}$  in the near-surface region and the bulk Fermi-level  $E_F$ . In semiconductors and insulators,  $\phi^{\hat{n}}$  refers to the ionization potential in which  $E_F$  is replaced by the valence-band maximum. Intuitively, the contribution to  $\phi^{\hat{n}}$  could be separated into an (unrelaxed) bulk part and a local surface relaxation part as shown in Fig. 1. However, a physically clear-cut definition of surface relaxation charges has been lacking for a long time because the bulk charges (and potentials) are continuously distributed and there is no clear “initial bulk configuration” to compare with the slab. In other words, a common reference to align the bulk to the vacuum before surface relaxation is missing here. Thus, the surface relaxation, which is defined from the differential charge between the relaxed slab and the initial bulk configuration, is a rather nontrivial issue. From a practical point of view, it means that we do not know what kind of truncated bulk should be used as the reference to define the surface relaxation.

Recently, some of the authors have identified the reference energy of periodic bulk as the *ideal vacuum* level [20], which is determined by truncating the bulk charge density by planar cuts at maxima of the average potential [see Figs. 1(a) and 1(c)]. In such truncated bulk, it is found that these maxima of the average potential are equivalent to the vacuum level, thus, can be used as the reference of a periodic bulk when aligned to the vacuum. Although the macroscopic monopole and dipole vanish in a periodic bulk due to charge neutrality and translational symmetry, the inhomogeneous distribution of bulk charge still provides a finite electric quadrupole tensor  $\mathbf{Q}$ . Across the surface of a truncated bulk with a given orientation  $\hat{n}$ , the commonly used bulk average electrostatic potential  $\bar{V}_{\text{bulk}}$  is offset from the ideal vacuum level  $V_{\text{ideal}}^{\hat{n}}$  by the potential associated with the quadrupole  $V_Q^{\hat{n}}$  [21],

$$\bar{V}_{\text{bulk}} = V_{\text{ideal}}^{\hat{n}} - V_Q^{\hat{n}} = V_{\text{ideal}}^{\hat{n}} - \frac{4\pi}{\Omega} \hat{n}^T \mathbf{Q} \hat{n}, \quad (1)$$

where  $\Omega$  is the unit-cell volume. Here, we decompose  $\phi^{\hat{n}}$  into a pure surface term plus a pure bulk term as

follows:

$$\begin{aligned} \phi^{\hat{n}} &= V_{\text{vac}}^{\hat{n}} - E_F \\ &= (V_{\text{vac}}^{\hat{n}} - V_{\text{ideal}}^{\hat{n}}) + (V_{\text{ideal}}^{\hat{n}} - E_F) \\ &= V_{D_R}^{\hat{n}} + \phi_I^{\hat{n}}, \end{aligned} \quad (2)$$

where  $V_{D_R}^{\hat{n}}$  is the surface relaxation dipole potential which shifts vacuum level from  $V_{\text{ideal}}^{\hat{n}}$  to  $V_{\text{vac}}^{\hat{n}}$ , whereas  $\phi_I^{\hat{n}}$  is the *innate bulk* work function, which is a pure bulk contribution to  $\phi^{\hat{n}}$ .

The innate bulk work function, defined as  $\phi_I^{\hat{n}} = V_{\text{ideal}}^{\hat{n}} - E_F$ , is related to the ideal vacuum level of bulk and can be straightforwardly calculated via a bulk unit cell.  $V_{D_R}^{\hat{n}}$ , however, is physically determined by the extent to which the self-consistent charge spills out into the vacuum region at a particular surface. As reflected schematically in Fig. 1(b), the truncated wave functions associated with electrons in bulk exponentially decay into the vacuum region with characteristic lengths which would depend on the difference in energies between their electronic states in the material and in the vacuum region. Considering a state at the Fermi level, before relaxation, this energy difference is simply  $\phi_I^{\hat{n}}$ . However, as charge spills out, the resulting surface dipole alters the alignment of the aforementioned states, yielding  $\phi^{\hat{n}}$ , which needs to be determined self-consistently.

### B. Model based on jellium approximation

Within the context of DFT calculation, the noninteracting electrons experience the same effective potential,

$$V_T(\mathbf{r}) = V_{\text{ion}}(\mathbf{r}) + V_H(\mathbf{r}) + v_{xc}(\mathbf{r}), \quad (3)$$

where the individual terms to the right correspond to the ionic electrostatic potential, the Hartree potential of electrons, and the exchange-correlation potential, respectively. In the work of LK [19], it was shown that the details of the ionic positions could be abstracted away and that the work function of simple metals are well described through a jellium approximation in which the ionic charge is assumed to be uniformly distributed. Although this approach has proved unsuccessful for nonmetals, it provides a picture of metals wherein the work function can be simply understood by the average electron density of the material.

Figures 2(a) and 2(b) schematically show the alignment between bulk and vacuum energy levels at the interface, before electronic relaxation, for a jellium system and an atomistic system, respectively. For the case of jellium, shown in Fig. 2(a), both the positive ionic charge and the negative electronic charge are uniformly distributed throughout the material (dark blue region). Therefore, the net charge vanishes everywhere, and the average electrostatic potential of the material equals that of vacuum  $\bar{V}_J = V_{\text{vac}}$ . Furthermore, as  $E_F$  of a uniform electron gas is above the vacuum level,  $\phi_I^{LK}$  is a negative quantity. For the case of an atomistic system, however, as depicted in Fig. 2(b), the ions are represented by point charges (or pseudopotentials designed to reproduce their affect) leading to charge inhomogeneity in the bulk region. For a planar cut of the charge density,  $V_{\text{vac}}^{\hat{n}}$  lines up with  $V_{\text{ideal}}^{\hat{n}}$ , and from Eq. (1), the average potential in the atomistic bulk region is distinct from the vacuum region by  $\bar{V}_{\text{bulk}} = V_{\text{vac}}^{\hat{n}} - V_Q^{\hat{n}}$ . In

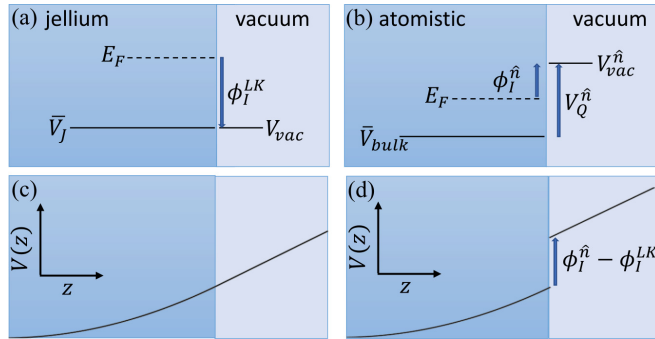


FIG. 2. Schematic of interfacial alignment between the truncated bulk and vacuum for (a) jellium and (b) atomistic system before surface relaxation. (c) Ionic potential of the jellium slab surface in (a). (d) The same as (c) but added by a surface step function to correct  $\phi_I$ .

this case,  $\phi_I^{\hat{n}}$  can be positive or negative, depending on the details of the material. It is important to note that in both cases, these level alignments are for the truncated material before surface electronic relaxation, and  $\phi_I$  is the driving force for charge spill out. Hence, whatever simplification to the problem is used, the accurate representation of  $\phi_I$  is necessary to obtain the appropriate physics.

In this context, LK's wide success for metals and failures for nonmetals can be understood. In particular, as systems become more metallic the details of the ionic coordinates are screened away and the electric quadrupole of the bulk system approaches zero. Hence, for metallic systems,  $\phi_I$  approach  $-E_F$  and the associated charge spill-out are well described by the jellium model. For semiconductors and insulators, on the other hand, as depicted in Fig. 2(b), the incomplete screening results in a significant electric quadrupole,  $V_Q^{\hat{n}}$ , which is not captured by jellium, leading to a  $\phi_I$  which can be entirely different than a metallic system of similar electron density.

This success of LK [19] for metals implies that jellium adequately describes the physics of surface charge relaxation, and the atomic details of the system are unimportant, provided the driving force for that spill-out  $\phi_I$  is accurate. As the jellium model of charge relaxation is so simple, it would be greatly beneficial if the approach could be extended to semiconductors and insulators. Our approach to accomplish this is to directly modify the jellium potential at the surface by adding a step potential which yields a jellium  $\phi_I$  equal to that of the semiconductor/insulator under investigation. This modification to the jellium potential in Fig. 2(c) is shown in Fig. 2(d). As the charge spill out is still calculated within the jellium approximation, but the potential is modified to correct  $\phi_I$ , we, hence, refer to it as the  $\phi_I$  corrected jellium ( $\phi_I J$ ) model. The procedure to determine the work function in the  $\phi_I J$  model is based on the relationship  $\phi = \phi_I + V_{Dr}$ , where  $\phi_I$  is determined from an atomistic calculation of the bulk solid.  $V_{Dr}$  is the surface dipole determined self-consistently from a calculation of a jellium slab with surface step potential  $\phi_I - \phi_I^{LK}$ .

### III. RESULTS AND DISCUSSION

To determine how well the relevant physics of the surface relaxation can be captured with such a simple jellium

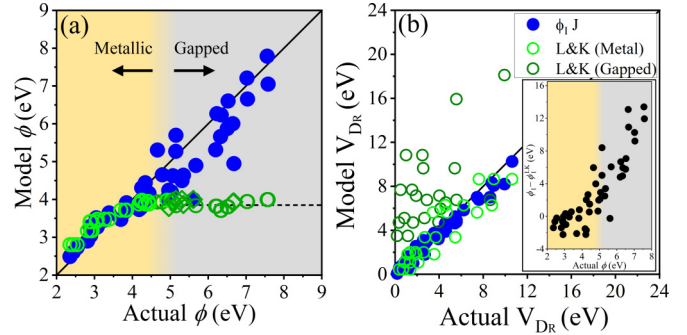


FIG. 3. (a) Calculated  $\phi$ , (b)  $V_{Dr}$ , and  $\phi_I - \phi_I^{LK}$  [the inset of (b)] for 21 metallic or gapped systems. The horizontal axis (actual) indicates the values obtained from fully atomistic DFT calculations. The vertical axis shows results of our  $\phi_I J$  model (blue shaded). The results from Lang and Kohn's approach [19] for metals (light-green open) and nonmetals (dark-green open) are included as a reference. Most materials are considered with more than one surface orientations ( $\hat{n}$ ), thus, the data points are more than 21.

approximation in the effective potential outlined above, we perform calculations on a series of 21 materials including face-centered-cubic structure elemental metals (Li, Na, K, Be, Mg, Ca, Al, and Ga), diamond/zinc-blende structure semiconductors (Si, BN, BeO, AlP, GaAs, and AlSb) and rock-salt structure insulators (LiF, LiBr, NaF, NaCl, KCl, MgO, and CaO). Our real-crystal calculations were performed using DFT by the VASP package [22] and exchange-correlation potential of local density approximation [23] with interactions between ion cores and valence electrons described by the projector augmented-wave (PAW) method [24]. Our jellium calculations were carried out by the GPAW package [25]. We used the optimized lattice structures from the Material Project Database [26] and fixed atomic positions for all the calculations. To simplify the discussion, we consider in this paper only the nonpolar surfaces for binary materials.

The results are summarized in Fig. 3 with comparison to the fully atomistic calculations. Here the horizontal axis corresponds to fully atomistic DFT calculation of the crystal (actual), whereas the vertical axis shows the values calculated from our  $\phi_I J$  model as well as LK's approach [19] (model). In Fig. 3(a) it can be seen that the  $\phi_I J$  model largely follows the diagonal line (corresponding to model  $\phi =$  actual  $\phi$ ) with some spread. The largest deviations are found for semiconductors in which the deviation can exceed 1 eV in the case of the (100) and (110) surfaces of Si and BN, respectively. For reference, the results from LK's approach [19] are shown by the open symbols. Although both methods work equally well for metallic systems as  $\phi$  becomes larger, LK's approach [19] predicts instead an almost constant  $\phi$  of nearly 4 eV. Note that larger  $\phi$  is also associated with the system developing an increasing band gap. As the gap becomes very large,  $\phi_I$  becomes critically important and the contribution of  $V_{Dr}$  can be understood as secondary response to  $\phi_I$ .

In Fig. 3(b) we directly compare this electron spill out within the  $\phi_I J$  model and LK's approach [19]. Although both using jellium to calculate the electron spill out and the corresponding surface dipole which develops, the  $\phi_I J$

model corrects the value of  $\phi_I$  within the jellium calculation so that the Fermi-level position relative to vacuum is well represented before considering the charge spill out. Here it can be seen that whereas the  $\phi_I J$  model largely reproduces the actual  $V_{Dr}$  across the range of metals, semiconductors, and insulators, LK's approach [19] for non-metals (dark-green open circles) generally leads to substantial overestimation.

In order to understand the general agreement of the two approaches for the case of *metals*, we examine the difference of  $\phi_I$  in the two approaches,  $\Delta\phi_I = \phi_I - \phi_I^{LK}$ , shown as an inset in Fig. 3(b) [note that  $\phi_I^{LK} = -E_F$  as depicted in Fig. 2(a)]. From the inset,  $\Delta\phi_I$  becomes large in gapped systems confirming the significant underestimation of  $\phi_I$  in LK's approach [19], which explains why it fails for semiconductors and insulators. In contrast,  $\Delta\phi_I$  is much smaller for metallic systems, thus, both approaches can work equally well in this range. The influence of ignoring  $\phi_I$  is much weaker in metallic systems so the relaxation dipole dominates, however, in semiconductors and insulators both  $\phi_I$  and  $V_{Dr}$  are non-negligible.

These results highlight the essential role of the ideal vacuum level in the understanding of the work function. Ideal vacuum level dictates how a periodic bulk lines up to actual vacuum and is a direct reflection of charge inhomogeneity under broken continuous translational symmetry, which manifests more intensely in semiconducting and insulating materials with highly localized bonds. Although all the direct structural information is removed in our jellium calculation, this effect of inhomogeneity is preserved by adequately accounting for  $\phi_I$ . Hence, the work function of both metals and nonmetals can be understood on the same footing.

Despite the success of the above description, we stress that  $\phi_I$  and the associated  $V_{Dr}$  are highly dependent on the orientation of the terminating surface. Although the orientation dependence of  $\phi_I$  and  $V_{Dr}$  largely cancel for the work-function  $\phi$ , within the  $\phi_I J$  model, consistent with the experimental observation (which typically exhibits direction dependence of less than 1 eV [27]). The origin of this large deviation in  $\phi_I$  can be traced back to our choice of a simple planar truncation of the surface. Depending on the orientation of the surface, such a cut can easily cut very close to the core of the atoms. Physically, we know that the charges should maintain both the translational symmetry (which has been preserved in our procedure) and rotational symmetry (or point group) of the crystal (which is violated by a planar cut). As such, a large part of the calculated surface relaxation is to restore the approximate rotational symmetry of bulk charge rather than relaxing with respect to the vacuum.

The use of a planar cut maintains  $V_{ideal} = V_{vac}$ , but this is not a requirement for the presented  $\phi_I J$  theory. In fact, it may be beneficial to perform a surface charge termination which more closely resembles the expected charge relaxation such that a sizable portion of the surface relaxation is incorporated in the bulk contribution to the work function,  $\phi_I'$ . In such a configuration, the periodic cell representing the bulk charge density has a shape distinct from the parallelepiped associated with the Bravais vectors. One such construction is the charge-neutral polyhedron (CNP) [28], which preserves both the translational and the rotational symmetry of the bulk crystal. In particular, a CNP is defined by partitioning the

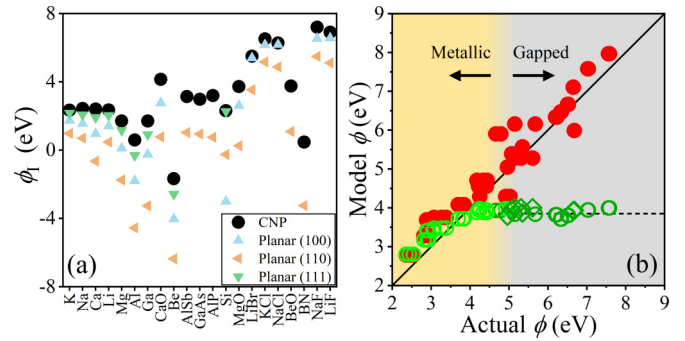


FIG. 4. (a) Comparison of  $\phi_I$  calculated using CNP cut (circles) and planar cut in different directions (triangles). The materials are ordered by ascending actual  $\phi$ . (b) The same as Fig. 3(a), but the results of the  $\phi_I J$  model (red shaded) are calculated using  $\phi_I$  obtained from the CNP cut. The result of Lang and Kohn's approach [19] (light-/dark-green open) is same as that in Fig. 3(a).

charge density into atom-centered charge-neutral polyhedra in a way similar to the determination of the Wigner-Seitz cell. One cuts real space with planes perpendicular to bonds between the target atom and all its neighbors with the distance to the plane determined such that the total charge enclosed in the smallest polyhedron vanishes for each atomic specie. For commonly studied elemental or binary materials, the CNP cell can be uniquely defined.

An interesting quality of the CNP partitioning for the materials studied here is that the innate work function  $\phi_I^{CNP}$  is completely *independent* of surface orientation. Comparison of  $\phi_I$  using the planar and CNP cut are shown in Fig. 4(a). Furthermore,  $\phi_I^{CNP}$  is consistently larger than  $\phi_I^{planar}$  because it is associated with a smaller relaxation dipole as it avoids cutting the charge density near the core region. Note that among the planar-cut directions, the (111) direction, which bisects nearest-neighbor bonds, yield results most similar to the CNP method. Despite the substantial differences in the cutting methods, they yield quite similar results for the work function when used in the  $\phi_I J$  model as shown in Figs. 3(a) and 4(b). Although there appears to be a mild systematic overestimation of  $\phi$  using the CNP cut, the results of nonmetals have been clearly improved. As  $\phi_I^{CNP}$  is orientation independent, this cut naturally yields an orientation-independent  $\phi$ , which, whereas only approximately true in experiment, is foundational in the chemical understanding of redox reactions and hints that the construction may have a deeper physical significance.

#### IV. CONCLUSIONS

To summarize, we have presented the  $\phi_I J$  model of the work function, where  $\phi_I$  is the bulk contribution to the work function, determined from the electrostatic quadrupole of the bulk solid. This  $\phi_I$  gives rise to a step potential at the surface. By including this discontinuity, we determine the additional surface contribution to the work function by a jellium model in which the atomistic details of the solid are replaced by the average density of bulk. This provides a unified understanding of the work function and its validity is shown over a wide range of metals, semiconductors, and insulators. These results

indicate that when the bulk contributions are adequately included, surface electronic relaxation can be well described by a simple model. As the work function is an extreme example of a material interface, this suggests that the interfacial dipoles can also be understood simply by bulk properties. This has large implications, especially in device physics where the interfacial properties are of paramount importance in determining device function.

## ACKNOWLEDGMENTS

S. Z. thanks D.-H. Choe for fruitful discussions. This work was supported by the US DOE Grant No. DE-SC0002623. The supercomputer time sponsored by National Energy Research Scientific Center (NERSC) under DOE Contract No. DE-AC02-05CH11231 and the Center for Computational Innovations (CCI) at RPI are also acknowledged.

- 
- [1] A. Einstein, *Ann. Phys. (NY)* **322**, 132 (1905).
  - [2] F. Huffman, *Encyc. Phys. Sci. Technol.* (3rd ed.) 627 (2003).
  - [3] C. T. Chan, K. M. Ho, and K. P. Bohnen, *Handbook Surf. Sci.* **1**, 101 (1996).
  - [4] S. R. Bare, and G. A. Somorjai, *Encyc. Phys. Sci. Technol.* (3rd ed.) 373 (2003).
  - [5] P. Bergveld, J. Hendrikse, and W. Olthuis, *Meas. Sci. Technol.* **9**, 1801 (1998).
  - [6] G. Hua and D. Li, *Phys. Chem. Chem. Phys.* **18**, 4753 (2016).
  - [7] H. Lu, Z. Liu, X. Yan, D. Li, L. Parent, and H. Tian, *Sci. Rep.* **6**, 24366 (2016).
  - [8] K. L. Jensen, D. W. Feldman, and P. G. O'Shea, *Free Electron Lasers 2002: Proceedings of the 24th International Free Electron Laser Conference and the 9th FEL Users Workshop*, Argonne, Illinois, U.S.A., September 9–13, 2002 (Elsevier B.V., Amsterdam, 2003).
  - [9] W. Schottky, *Z. Phys.* **113**, 367 (1939).
  - [10] N. Mott, *Proc. R. Soc. London, Ser. A* **171**, 27 (1939).
  - [11] R. L. Anderson, *IBM J. Res. Develop.* **4**, 283 (1960).
  - [12] H. Kroemer, Heterostructures for Everything? in *Lindau Nobel Laureate Meeting* (2001).
  - [13] A. Kahn, *Mater. Horiz.* **3**, 7 (2016).
  - [14] D. Y. Li, L. Guo, L. Li, and H. Lu, *Sci. Rep.* **7**, 9673 (2017).
  - [15] K. Sivula, and R. van de Krol, *Nat. Rev. Mater.* **1**, 15010 (2016).
  - [16] S. De Waele, K. Lejaeghere, M. Sluydts, and S. Cottenier, *Phys. Rev. B* **94**, 235418 (2016).
  - [17] X. Ma, Y. Dai, L. Yu, and B. Huang, *Nanoscale* **8**, 1352 (2016).
  - [18] R. T. Tung, *Appl. Phys. Rev.* **1**, 011304 (2014).
  - [19] N. D. Lang and W. Kohn, *Phys. Rev. B* **3**, 1215 (1971).
  - [20] D.-H. Choe, D. West, and S. Zhang, *Phys. Rev. Lett.* **121**, 196802 (2018).
  - [21] D.-H. Choe, D. West, and S. Zhang, *Phys. Rev. B* **103**, 235202 (2021).
  - [22] G. Kresse and J. Furthmüller, *Phys. Rev. B* **54**, 11169 (1996).
  - [23] D. M. Ceperley and B. J. Alder, *Phys. Rev. Lett.* **45**, 566 (1980).
  - [24] P. E. Blöchl, *Phys. Rev. B* **50**, 17953 (1994).
  - [25] J. Enkovaara, C. Rostgaard, J. J. Mortensen, J. Chen, M. Duřak, L. Ferrighi, J. Gavnholt, C. Glinsvad, V. Haikola, H. A. Hansen *et al.*, *J. Phys.: Condens. Matter* **22**, 253202 (2010).
  - [26] A. Jain, S. P. Ong, G. Hautier, W. Chen, W. D. Richards, S. Dacek, S. Cholia, D. Gunter, D. Skinner, G. Ceder *et al.*, *APL Mater.* **1**, 011002 (2013).
  - [27] R. Tran, X. G. Li, J. H. Montoya, D. Winston, K. A. Persson, and S. P. Ong, *Surf. Sci.* **687**, 48 (2019).
  - [28] R. T. Tung and L. Kronik, *Phys. Rev. B* **94**, 075310 (2016).